Available online at www.sciencedirect.com

SCIENCE DIRECT®

Thin Solid Films 484 (2005) 379–381

thin solid films

www.elsevier.com/locate/tsf

Effect of distribution of field enhancement factor on field emission from cathode with a large number of emission sites

Guang Yuan[a,b,*], Hang Song[b], Yixin Jin[b], Hidenori Mimura[c], Kuniyoshi Yokoo[c]

[a] *School of Information Science and Engineering ,Ocean University of China, No.23 HongKong East Road, QingDao City 266071, China*
[b] *Changchun Institute of Optics, Fine Mechanics and Physics, Chinese Academy of Sciences, Changchun 130022, China*
[c] *Research Institute of Electric Communication, Tohoku University, Katahira 1-1-1, Aobaku, Sendai 980-8577, Japan*

Received 14 January 2003; accepted in revised form 24 January 2005
Available online 5 March 2005

Abstract

In this paper, the electron emission from a cathode with a large number of emission sites is discussed by introducing a distribution function of the field enhancement factor β. After accounting for the distribution of the field enhancement factor, the field electron emission from the cathode deviates from the classical Fowler–Nordheim (F–N) theory, the F–N plot is not a straight line and bends up in region of low electric field. A good agreement of the calculated results with experimental results was achieved by employing a reasonable distribution function of β.

PACS: 116; 94; 146; 462
Keywords: Fowler–Nordheim theory; Field enhancement factor (FEF); Distribution of FEF

1. Introduction

Vacuum microelectronics has attracted much interest in the field of electron devices due to its high potential application [1–4]. A cathode with a large number of emission sites usually favours the increase and stabilization of the emission current. Besides conventional field emitters, such as Spindt-type metal emitters [5] and Si conical emitters [6], many kinds of new emitters including carbon nanotube [7], polycrystalline diamond [8] and porous Si [9] are intensively studied to achieve a high and stable emission current. However, in some case, the emission characteristics experimentally observed do not follow the classical Fowler–Nordheim (F–N) theory [8,10–12], and several reasons for this disagreement have been suggested, such as space charge [13] and three-dimensional effect [14,15]. Diamond and related materials are strong candidates as cold cathode materials, but there is a large difference in emission characteristics observed by different groups and the emission mechanism is still far from being understood. One of the reasons for variation among the reported results of emission characteristics may be non-uniformity or scatter in geometrical shape of emission sites.

This paper discusses the effect of scatter in the geometrical shape of emission site for an emitter with a large number of emission sites by introducing a distribution function in field enhancement factor β. In addition, the paper shows that the calculated results agree well with the experimental results obtained in molybdenum emitter arrays coated with diamond-like carbon by employing a reasonable distribution of β.

* Corresponding author. School of Information Science and Engineering, Ocean University of China, No.23 HongKong East Road, QingDao City 266071, China. Tel./fax: +86 532 5901204.
E-mail address: yuanguang@ouc.edu.cn (G. Yuan).

0040-6090/$ - see front matter © 2005 Elsevier B.V. All rights reserved.
doi:10.1016/j.tsf.2005.01.086

2. Calculation model

The total emission current J for an emitter with a large number of emission sites can be expressed as the sum of emission current from the individual emission site,

$$J(E) \equiv \sum_{1}^{N_0} j_i(E) \tag{1}$$

where E is the average field, defined as value of the gate voltage divided by the gate-emitter distance for a triode structure, or the anode voltage divided by the anode-emitter distance for a diode structure, j_i (E) is the emission current from one of the emission sites and N_0 is the total number of emission sites.

When the electric field is not uniform over the area of an emission site, the j_i (E) is expressed as an integral formula,

$$j_i(E) = \int_0^{S_i} j_0(F_i) \cdot dS(F_i) \tag{2}$$

where F_i is the electric field on the surface of emission site, S_i the emission area of the emission site, and j_0 the emission current density given by Fowler–Nordheim formula as shown in the following,

$$j_0(F_i) = \frac{1.54 \times 10^{-6} F_i^2}{\phi} e^{\left(6.83 \times 10^7 \frac{\phi^{1.5}}{F_i}\right)} \tag{3}$$

where ϕ is the work function in eV.

Usually the field electron emission easily occurs at a sharp tip called emission site. The electric field at the emission site is generally enhanced over the average electric field by a factor according to the geometrical structure of the individual emission site and the factor is almost inversely proportional to the curvature radius of the tip of the emission site. Then, the electric field on the surface of emission site is simply taken as $F_i = \beta_i \cdot E$, where β_i is the field enhancement factor of an emission site and E is the average electric field as defined above.

After introducing the field enhancement factor, Eq. (2) can be simplified for individual emission sites as,

$$j_i(E) = j_0(\beta_i, E) \cdot S_i(\beta_i) \tag{4}$$

where $j_0(\beta_i, E)$ and $S_i(\beta_i)$ are the current density and the emission area for an emission site with a field enhancement factor β_i, respectively. Furthermore, β_i is almost inversely proportional to the curvature radius of the tip of emission site, the emission area $S_i(\beta_i)$ is simply assumed to be a quarter of spherical surface and then to be inversely proportional to the square of β_i. Then, Eq. (4) becomes

$$j_i(E) = 1.54 \times 10^{-6} \times \pi \frac{d^2}{\phi} E^2 e^{\left(-6.83 \times 10^7 \frac{\phi^{1.5}}{\beta_i E}\right)} \tag{5}$$

where d is the distance between emitter and gate for a triode or emitter and anode for a diode structure.

It is reasonable that the β_i varies in every emission site depended on their geometrical structure and distributes surrounding a certain value. Therefore, we introduce a distribution function of $N(\beta)$ for the scatter of β, and Gaussian distribution is accessible for $N(\beta)$.

Finally, the total current can be expressed by following,

$$J(E) \equiv \int_1^{\infty} 1.54 \times 10^{-6} \times \pi \frac{d^2}{\phi} E^2 e^{\left(-6.83 \times 10^7 \frac{\phi^{1.5}}{\beta E}\right)} \cdot N(\beta) \cdot d\beta \tag{6}$$

where the $J(E)$ is the total current in mA, E is average field in V/cm, d in cm and ϕ in eV.

Here, the effects of image force and three-dimension on electron tunneling was neglected for simplification.

3. Results and discussions

Fig. 1 shows the F–N plots of the calculated results under various Gaussian distribution of β as shown in following, and the work function ϕ was taken as 4 eV as a conventional emitter material,

$$N(\beta) \equiv \frac{N_0}{C} \exp\left(-\frac{2 \times (\beta_0 - \beta)^2}{w^2}\right) \tag{7}$$

where the centre value of β is 200 denoted as β_0 and the full width at half maximum (FWHM) of the distribution function, w, are taken in 100, 200 and 400, respectively. Although the Gaussian distribution spreads out into negative values, here the values larger than 1 were employed in the calculation and the normalization constant C of each distribution was determined for the β value larger than 1. As shown in Fig. 1, Gaussian distribution of β modified the F–N plots from a conventional straight line and bended up especially in low field region. The straight lines extracted from high field region are also shown in Fig. 1 for the

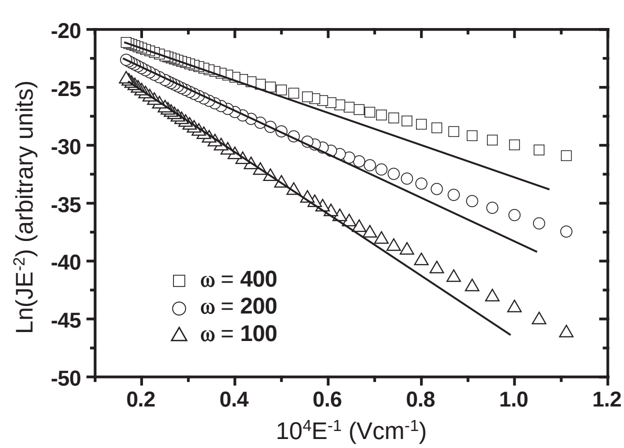

Fig. 1. The calculation results of the F–N plots under Gaussian distribution β_0=200 and w=100, 200 and 400, respectively. The straight lines are extracted directly from the calculated F–N plots in high field region.

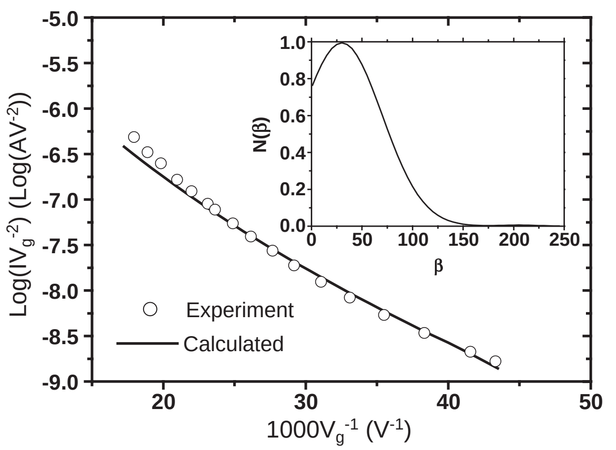

Fig. 2. The experimental and calculated F–N plot, inset, is the suitable distribution $N(\beta)$ used for calculation, $N(\beta) = 0.994\exp\left(\frac{(\beta-30)^2}{3200}\right) + 0.006\exp\left(\frac{(\beta-205)^2}{800}\right)$.

comparison. The bending in the F–N slop observed in the low electric field becomes remarkable with increase in w. Because the emission sites with high β values mainly contribute to total emission current in the low electric field, while in the high field many numbers of the emission sites with low β values contribute to the emission current, a deviation of the F–N plots from a straight line can be expected. A straight line in F–N plot, observed experimentally in Spindt emitters and other materials including diamond films and nano-tube carbon, may be the result of the narrow distribution in β, or the emission from only a few emission sites with similar β value.

The bending in F–N plots at low field have been observed experimentally by Jung et al. [11], who has carried out measurements using a molybdenum Spindt emitter with 1200 tips coated with 20 nm thick DLC. The F–N plot was fitted by employing a reasonable Gaussian distribution, as shown in Fig. 2, where the work function of DLC was taken as 3 eV from our previous experiments [16]. The distribution of β used in the calculation is shown in the inset in Fig. 2. As shown in Fig. 2, both calculation and experimental results agree well especially at low electric field, though the calculation deviates slightly from the experiment in the high field region. The distribution of β is acceptable considering of the actual emitter configuration. In addition, the calculation suggests that the DLC coating increase the emission sites by about 1.25 times compared with that of Mo emitter tips. The above results indicate the variation in emission properties of diamond films and/or DLC come partly from non-uniformity in geometrical shape between emission sites. Especially, the bending in F–N plots is more apparent in the low field region as shown in Fig. 1, in other words, the field emission from DLC is observed in low electric field region and that indicates there is a large potential to obtain a high emission current from DLC at higher field.

Then, the distribution of β is useful to describe the scatter in geometrical structure of the emission sites. A simple way to measure the distribution of β experimentally is to observe the images of the emitted electron impacted on a phosphoresce screen and count the number of emission spots for the respective brightness [17,18], since the emission sites with large β illuminate the phosphor at low electric field, while that with smaller β appear at high field.

On the other hand, the work function of individual emission site varies by absorption and contamination of gas molecules, and there is a distribution of work function among electron emission sites. The effect of the distribution of work function on electron emission from cathode with a large number of emission sites can be treated by the similar way as above.

4. Conclusion

The field emission from cathode with a large number of emission sites was discussed by introducing a distribution function of field enhancement factor β. The F–N plots will deviate from a conventional straight line especially at low electric field. The calculation results based on the model shows to agree fairly well with the experimental results and are able to explain the emission behaviour of a field emission from cathode with a large emission sites.

References

[1] K. Sawada, IEEE Trans. Electron Devices ED-45 (1998) 321.
[2] M. Tani, S. Matsuura, K. Sakai, S. Nakashima, Appl. Opt. 36 (1997) 7853.
[3] H. Makishita, S. Miyano, H. Imura, J. Matsuoka, H. Takemura, A. Okamoto, Appl. Surf. Sci. 146 (1999) 230.
[4] J. Itoh, K. Uemura, S. Knemaru, J. Vac. Sci. Technol., B 16 (1998) 1233.
[5] C.A. Spindt, I. Brodie, L. Humphrey, E.R. Westerberg, J. Appl. Phys. 47 (1976) 5248.
[6] K. Yokoo, M. Arai, M. Mori, J. Bae, S. Ono, J. Vac. Sci. Technol., B 13 (1995) 491.
[7] W.A. de Heer, A. Chaelain, D. Ugarte, Science 270 (1995) 1179.
[8] K. Okano, S. Koizum, S.R.P. Silva, G.A.J. Amaratunga, Nature 381 (1996) 140.
[9] T. Komoda, X. Sheng, N. Koshid, J. Vac. Sci. Technol., B 17 (1999) 1076.
[10] R.H. Fowler, L.W. Nordheim, Proc. R. Soc. Lond, A 119 (1928) 173.
[11] J.H. Jung, B.K. Ju, H. Kim, J. Vac. Sci. Technol., B 16 (1998) 705.
[12] J. Chen, S.Z. Deng, N.S. Xu, K.H. Wu, E.G. Wang, Appl. Phys. Lett. 75 (1999) 1323.
[13] W.A. Anderson, J. Vac. Sci. Technol., B 11 (1993) 383.
[14] P.H. Culter, J. He, N.M. Miskovsky, T.E. Sullivan, B. Weiss, J. Vac. Sci. Technol., B 11 (1993) 387.
[15] G.N. Furseyd, D.V. Glazanov, J. Vac. Sci. Technol., B 16 (1998) 910.
[16] H. Mimura, G. Hashiguchi, M. Okada, J. Appl. Phys. 84 (1998) 3378.
[17] O. Groning, O.M. Kuttel, P. Groning, L. Schlapbach, J. Vac. Sci. Technol., B 17 (1999) 1970.
[18] B. Cui, J. Robertson, W.I. Milne, J. Appl. Phys. 89 (2001) 5707.